Identification of neural and non-neural contributors to joint stiffness in upper motor neuron disease

Gooijer-van de Groep, K.L. de

Cover Page

Universiteit Leiden

The following handle holds various files of this Leiden University dissertation:
http://hdl.handle.net/1887/74470

Author: Gooijer-van de Groep, K.L. de
Title: Identification of neural and non-neural contributors to joint stiffness in upper motor neuron disease
Issue Date: 2019-06-20

CHAPTER 4

Estimation of tissue stiffness, reflex activity, optimal muscle length and slack length in stroke patients using an electromyography driven antagonistic wrist model

Authors:
Karin L. de Gooijer-van de Groep, Erwin de Vlugt,
Hanneke J. van der Krogt, Áróra Helgadóttir, J. Hans Arendzen,
Carel G.M. Meskers, Jurriaan H. de Groot
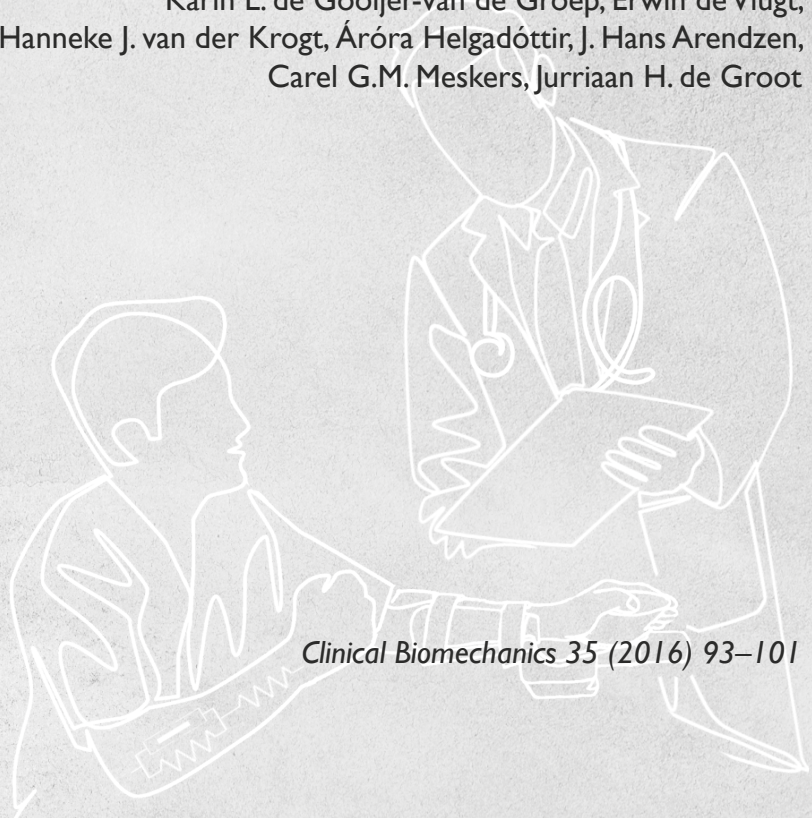
Abstract

About half of all chronic stroke patients experience loss of arm function coinciding with increased stiffness, reduced range of motion and a flexed wrist due to a change in neural and/or structural tissue properties. Quantitative assessment of these changes is of clinical importance, yet not trivial. The goal of this study was to quantify the neural and structural properties contributing to wrist joint stiffness and to compare these properties between healthy subjects and stroke patients.

Stroke patients ($n=32$) and healthy volunteers ($n=14$) were measured using ramp-and-hold rotations applied to the wrist joint by a haptic manipulator. Neural (reflexive torque) and structural (connective tissue stiffness, optimal muscle lengths and slack lengths of connective tissue) parameters were estimated using an electromyography driven antagonistic wrist model. Kruskal-Wallis analysis with multiple comparisons was used to compare results between healthy subjects, stroke patients with modified Ashworth score of zero and stroke patients with modified Ashworth score of one or more.

Stroke patients with modified Ashworth score of one or more differed from healthy controls ($P<0.05$) by increased tissue stiffness, increased reflexive torque, decreased optimal muscle length and decreased slack length of connective tissue of the flexor muscles.

Non-invasive quantitative analysis, including estimation of optimal muscle lengths, enables to identify neural and non-neural changes in chronic stroke patients. Monitoring these changes in time is important to understand the recovery process and to optimize treatment.

Introduction

Movement disorders of central neurological origin, like stroke and cerebral palsy, are characterized by increased resistance to imposed movement in the relaxed condition. Increased joint stiffness can be of neural origin (hyperreflexia, "spasticity") and/or non-neural, structural origin (altered tissue viscoelastic properties, "contracture")[1;2]. Separation of joint stiffness into neural and non-neural contributions has gained much attention recently, both from technical and clinical research, resulting in new and promising instrumented methods[2;3]. The separation of joint stiffness into different components is important for treatment selection aiming to improve joint dexterity. In case of suspected neural origin, botulinum toxin may be administered[4;5], while in case of suspected non-neural origin patients may benefit from corrective casting, splinting or surgical lengthening[6-8]. The use of an instrumented joint manipulator and an electromyography driven biomechanical model was successfully used previously to quantitatively discriminate joint stiffness into contributions from connective tissue viscoelasticity and stretch reflex activity in the ankle of patients with stroke[9] and cerebral palsy[10;11].

About half of all stroke survivors experience loss of arm function[12;13] often due to a flexed position of the wrist at the affected side due to developing contractures at about 0.5 degrees per week in the first 8 months post-stroke[14]. The origin of these contractures is not fully clear, but may be the result of reduced number of sarcomeres in series[15-18] and/or shortened optimal sarcomere length[17], increased stiffness of the extracellular matrix[18], functional immobilization[14;19] and co-activation synergies[20]. Biomechanically, these tissue changes mean a shift in slack length of the connective tissues and/or shift of the muscle force-length curve and a reduction of the optimal muscle length of the flexor muscles, i.e. the length of the muscle where it generates highest forces.

In the acute and sub-acute phase post-stroke, quantification of neural and non-neural contributors to joint stiffness, including optimal muscle length and slack length of connective tissue, could help understanding the mechanism of (poor) recovery after stroke and characterization of changes over time using longitudinal observations[21;22]. Also the effect of therapies, like botulinum toxin, on the neural and non-neural parameters is not yet understood and should be measured to evaluate and optimize treatment[23].

The goal of this study was to quantify the neural and non-neural contributions to wrist joint stiffness from both flexor and extensor muscles in a cohort of chronic stroke patients. The current model is an extended version of a previous ankle model[9] now including an antagonistic pair of muscle elements to allow for property analysis of both wrist flexor and extensor muscle groups. Three demands were imposed to the model: The structure of the model should represent the (non-linear) joint physiology, the predicted torques should resemble the measured torques and the parameters should be sensitive to discriminate clinical different patients from healthy subjects. Optimal muscle lengths, slack muscle lengths, tissue stiffness and reflexive torques from both flexor and extensor muscles were estimated by model optimization and compared between healthy subjects, stroke patients with a modified Ashworth score of 0 (MAS = 0) and stroke patients with modified Ashworth score of one or more (MAS ≥ 1). We hypothesized an increase in tissue stiffness and reflexive torque and decrease of optimal muscle length and slack length of connective tissue of the flexor muscles in chronic stroke patients with modified Ashworth score of one or more (MAS ≥ 1). We addressed the validity and agreement of the method.

Methods

Subjects

Instrumented ramp-and-hold (RaH) measurements at the wrist at rest were performed as part of the EXPLICIT-stroke study[21;24;25]. Exclusion criteria were neurological deficiencies additional to stroke, (prior) orthopedic problems in hand or shoulder and inability to comply with the protocol. Patients were measured on two occasions within a month. Healthy volunteers were measured as a reference group. The study was approved by the medical ethics committee of the Leiden University Medical Center. All participants gave their written informed consent prior to the experimental procedure. Measurements from fourteen healthy volunteers (mean age 49.4, SD 15.1 years), 21 chronic stroke patients with MAS = 0 (mean age 60.4, SD 13.1 years) and 11 chronic stroke patients with MAS ≥ 1 (mean age 54.4, SD 12.7 years) were analyzed in this study. Subject characteristics are provided in Table 4.1.

Table 4.1: *Subject characteristics[25]*

	Healthy volunteers (n=14)	Chronic patients MAS = 0 (n = 21)	Chronic patients MAS ≥ 1 (n = 11)
Age (years) (SD)	49.4 (15.1)	60.4 (13.1)	54.5 (12.7)
Men (n) (%)	9 (64%)	10 (48%)	3 (27%)
Right side dominant (n) (%)	13 (93%)	21 (100%)	8 (73%)
Measured side dominant (n) (%)	14 (100%)	10 (48%)	4 (36%)
Time between measurements (days) (SD)	27 (21)	18 (7)	29 (17)
Time after stroke (months) (SD)	-	30 (27.6)	53 (34.4)
Age at moment of stroke (years) (SD)	-	58 (13.1)	50 (14.5)
Passive range of motion deg,(median min;max)	138 (118; 148)	132 (100; 151)	100 (42; 133)

Instrumentation

The subjects were seated with their shoulder relaxed and elbow flexed in approximately 90°. A haptic wrist manipulator (Wristalyzer, 1 degree of freedom (dorsi- and plantar flexion), Moog, Nieuw Vennep, the Netherlands) was used (Figure 4.1). Forearm and hand were strapped to a cuff and handle respectively using Velcro straps. The rotation axis of the wrist joint was aligned visually to the rotation axis of the handle. Handle rotation was driven by a vertically positioned servo motor (Parker SMH100). Positive direction was assigned to flexion movement and extension torque. Muscle activation was recorded by bipolar surface electrodes (electromyography, EMG) using a Delsys Bagnoli 8 system (Delsys Inc., Boston MA, USA). Two bipolar electrodes were placed on the flexor carpi radialis (FCR) and two on the extensor carpi radialis (ECR) in order to have a good representation for the FCR and ECR activation[26;27]. EMG signals were sampled at 2048 Hz, online band pass filtered (20-450 Hz), rectified and low pass filtered (20 Hz, 3rd order Butterworth) to obtain the EMG envelope. The minimal EMG value (average of moving window of 0.06 sec) was subtracted from the total EMG to ensure

noise was minimal in the data. Wrist torque and joint angle were recorded at 2048 Hz and filtered with the same 20 Hz low pass 3rd order Butterworth filter.
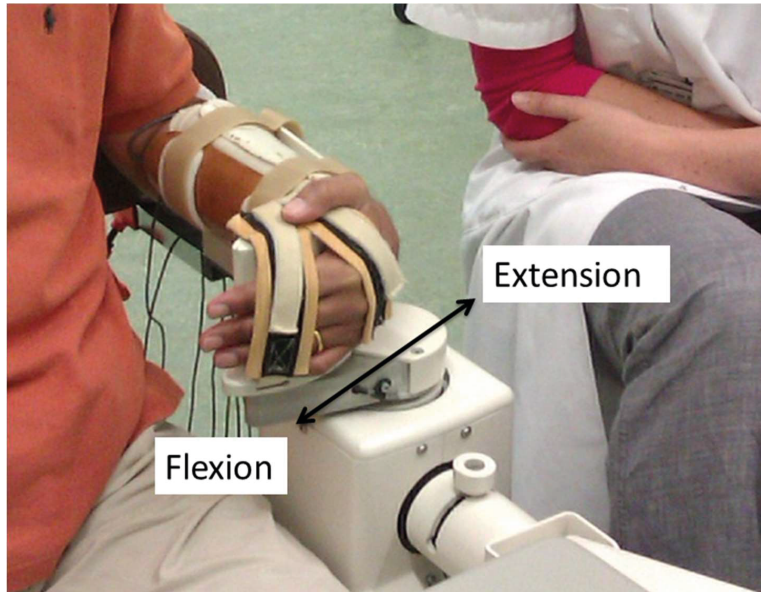
Figure 4.1: *Experimental setup. The forearm and hand of the subject were fixed to the manipulator (Wristalyzer® by MOOG, the Netherlands). Ramp-and-hold rotations in flexion and extension were imposed to the wrist while the subject was instructed to remain relaxed and not react to the rotations. Wrist joint torque, angle and EMG of the FRC and ECR muscles were recorded.*

Measurement protocol

Measurements were performed on the right wrist in healthy subjects and on the impaired wrist in patients. The range of motion (RoM) was determined as the difference between maximal flexion and extension angle resulting from an imposed slow changing torque ranging between 2 Nm (extension torque) and –2 Nm (flexion torque). Subsequently, RaH rotations were imposed onto the wrist at a constant velocity over the full RoM. Two RaH trials were imposed per measurement. Each trial contained a fast ramp in 1 second in extension or flexion direction (named "extension fast" or "flexion fast"), two slow ramps in the opposite direction and three hold periods in between the ramps in which the position of the wrist stayed the same (Figure 4.2). The directions of the ramps in the second trial were opposite to the first trial. The individually determined RoM in combination with the duration of the ramp (1 second)

determined the velocity of the imposed perturbations. Subjects were asked to remain relaxed during the entire experiment and not to react to the wrist movement.
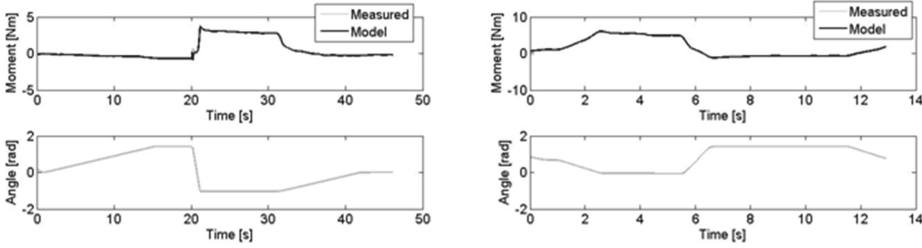
Figure 4.2: *Example of imposed angular rotation (bottom) and torque response with model fit (top row) for a healthy subject (left, "extension fast", VAF=99.6%) and stroke subject with MAS=3 (right, "flexion fast", VAF=99.8).*

Model description

A biomechanical EMG driven antagonistic muscle model was used to predict wrist torque from wrist angle and EMG. The model was based on the ankle model from de Vlugt et al.[9] and extended with a second Hill-type model to describe the passive and active force of the antagonist muscles.

Wrist joint stiffness is described by:

$$T_{mod}(t) = I\ddot{\theta}(t) + T_{ext}(t) - T_{flex}(t) \qquad (4.1)$$

where t is the independent time variable [s], T_{mod} the modeled wrist reaction torque [Nm], $\ddot{\theta}(t)$ the wrist angular acceleration [rad/s^2], I the inertia of wrist and handle [kg.m^2], T_{ext} the torque generated by the extensor muscles [Nm] and T_{flex} the torque generated by the flexor muscles [Nm].

Muscle torques (T_m) for extensor and flexor muscle are described by:

$$T_m(\theta,t) = (F_{elas,m}(l) + F_{act,m}(v_m, l_m, \alpha_m))r_m(\theta) \qquad (4.2)$$

with $F_{elas,m}$ the elastic force of the parallel connective tissues [N], $F_{act,m}$ the active or "reflexive" muscle forces [N] according to the Hill-type model, v_m the muscle lengthening velocity [m/s], l_m the muscle length [m], α_m the active state [-] and $r_m(\theta)$ the angle dependent moment arm [m] of the tendon.

The elastic components for the extensor and flexor muscles were modeled as follows:

$$F_{elas,m}(t) = e^{k_m(l_m(\theta) - l_{p,slack,m})} \tag{4.3}$$

Where k_m is the estimated stiffness coefficient of the muscle and $l_{p,slack,m}$ the estimated slack length of the connective tissue. Muscle length l_m for FCR and ECR equals:

$$l_{FCR} = l_{FCR,0} - r_{FCR}(\theta) * \theta \tag{4.4}$$

$$l_{ECR} = l_{ECR,0} + r_{ECR}(\theta) * \theta \tag{4.5}$$

Where l_{FCR} and l_{ECR} are the lengths of the muscle at each position θ and $l_{FCR,0}$ and $l_{ECR,0}$ the muscle length at zero degrees wrist angle position (handle in line with forearm). r_m is the moment arm defined by Ramsay et al.[28].

The Hill-type muscle model was used to compute the muscle force from the active state and the muscle length and velocity according to:

$$F_{act,m} = f_v(v_m) f_l(l, l_{opt,m}) \alpha_m \tag{4.6}$$

with f_v the force-velocity relationship and f_l the force-length relationship.

The optimal muscle lengths ($l_{opt,m}$) were estimated using the model and used to derive the force-length relationships by

$$f_l = e^{-\left(l_m - l_{opt,m}\right)^2 / w_{fl,m}}$$ (4.7)

With $w_{fl,m}$ a shape factor.

The complete model is described in the Appendix 4.

The modeled force-length and force-velocity characteristics are shown in Figure 4.3 together with the modeled tissue and neural forces. In estimating the optimal muscle lengths, the active filament overlap component was decoupled from the passive component, i.e. the slack length of the muscle which is often assumed to be equal to the optimal muscle length[29-31] was decoupled. The parameters of the wrist model that were optimized including the initial values and constraints are listed in Table 4.2.

Table 4.2: *Estimated model parameters and optimization parameters.*

Model wrist	Description	Initial value and [Min Max] of optimization			
M	Mass (kg)	2	[0.5-5]		
k_{ext}, k_{flex}	Stiffness coefficients (1/m)	240	[10 800]	230	[10 800]
$l_{p,slack,ext}$, $l_{p,slack,flex}$	Slack lengths of connective tissue (m)	0.06	[-0.1 0.1]	0.04	[-0.1 0.1]
G_{ext}, G_{flex}	EMG weighting factors (-)	$1*10^4$	$[1*10^0\ 1*10^{11}]$ (both muscles)		
f_0	Activation cutoff frequency (Hz)	0.2	[0.01 10]		
$l_{opt,ext}$, $l_{opt,flex}$	Optimal muscle lengths (m)	0.070	[0.04 0.11]	0.063	[0.04 0.11]
tau_{rel}	Tissue relaxation time constant (s)	0.9	[0 10]		
k_{rel}	Tissue relaxation factor (-)	1	[0 50]		
12	(Number of parameters)				
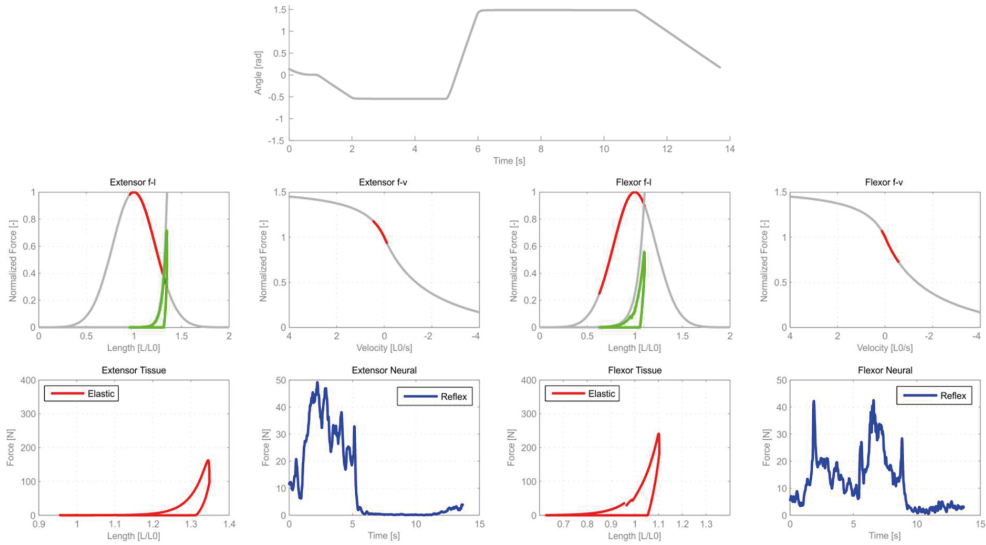
Figure 4.3: *Example of model characteristics of a stroke patient (MAS = 0). Top panel: applied movement, second row: normalized force-length and force-velocity curves of the extensor (left) and flexor (right) muscles (grey lines) including the perturbed length and velocity domains by the red and green intervals. Bottom row: Tissue and neural forces from the extensor (left) and flexor (right) muscles.*

The predicted model torque (T_{mod}) was fitted to the measured wrist torque (T_{meas}), except for the first second of the data to ensure data quality. Model parameters were estimated for the complete movement by minimizing the quadratic difference (error function) between the measured and predicted wrist torque using a non-linear least-square optimization algorithm (steepest descent, Matlab function lsqnonlin).

The main estimated outcome measures used to characterize subjects were tissue stiffness at joint level (K_{joint}), optimal muscle length ($l_{opt,m}$), slack muscle length ($l_{p,slack,m}$) and the reflexive torque (T_{reflex}) determined for both the extensor and flexor muscle groups. The estimated reflexive torque was calculated by using the root mean square of the active muscle torque[9]. Tissue stiffness at joint level (K_{joint}) was derived from the passive force-length relationship, see Appendix 4. For clinical comparison between subjects, K_{joint}, was compared at the same wrist

angle (θ_{comp}) for all subjects. This angle was chosen at zero degrees, i.e. where the handle is in line with the forearm.

Repeated measures were averaged for each subject in order to be able to compare groups of subjects.

Simulation and analysis was performed in Matlab (The Mathworks Inc., Natick MA).

Validity and agreement

Model validity was assessed using the standard error of the mean (SEM) and variance accounted for (VAF). Validity of the measurements was determined by systematic error assessment. Agreement of measurement[32] was determined by the minimal detectable change (MDC) and was used to assess clinical potential to discriminate pathological deviating parameters from normal values.

Model fit and parameter confidence
The standard error of the mean (SEM) represents the parameter confidence and is based on the sensitivity (first and second partial derivatives) of each parameter to the error function (Jacobian and Hessian respectively)[9;33]. High sensitivity, indicated by low SEM values, means that the parameter has substantial contribution to the error function. Model fit was indicated by the torque variance accounted for (VAF):

$$VAF = \left(1 - \frac{\sum\left((T_{meas}(t) - T_{mean}(t)) - (T_{mod}(t) - T_{mean}(t))\right)^2}{\sum(T_{meas}(t) - T_{mean}(t))^2}\right) * 100\% \quad (4.8)$$

The VAF was estimated for each trial. Estimated torques with a VAF less than 98% were disregarded from group analysis.

Assessment of systematic error

A Wilcoxon signed rank test with significant level 0.05 was used to determine systematic errors between the measurements of two different visits.

Clinical potential

Using post-hoc analysis based on variance (Levene's test) we observed significant higher parameter variances in stroke patients compared to controls for the tissue stiffness and reflexive torque of the FCR. Conform the analysis of[25] we introduced an a priory subdivision of stroke patients based on MAS.

Kruskal-Wallis one-way analysis of variance with multiple comparisons was used to compare stroke patients with modified Ashworth scores of 0 (MAS = 0) and greater than 0 (MAS ≥ 1) respectively with healthy subjects. The minimal detectable change (MDC)[32;34] with confidence interval of 95% was calculated to identify deviated parameters i.e. parameters that are outside the range of mean value +/- MDC indicating that the observed value was not likely to be due to chance variation. Thus, values above the threshold of mean value +/- MDC were classified as "deviated" and can be used to identify pathological cases.

For statistical analysis IBM SPSS statistics 22 and GraphPad Prism 6 was used.

Results

One patient was unable to comply with the protocol. All other trials (93 in "extension fast" direction and 93 in "flexion fast" direction were used to estimate model parameters, VAF and SEM values (Table 4.3). Twenty trials (10%, 5 (5%) in "extension fast" and 15 (16%) in "flexion fast" direction) were excluded for further analysis based on VAF values below 98% and in one case (1 of 93, "extension fast") the input signal was corrupt. In only one (out of 45) subject, the parameters could not be estimated because the patient had low VAF values in both movement direction and for both trials. From all other subjects, through repeated trials in flexion and extension, data were available to estimate the relevant parameters. In total data from 14 healthy subjects and 30 stroke were used for further analysis. Low VAF values may have originated from experimental artefacts e.g. poor fixation or misalignment or voluntary interaction with the passive protocol.

Table 4.3: *Model parameters (estimated value and standard error of the mean (SEM)) for all healthy subjects (A), stroke patients with MAS = 0 (B) and stroke patients with MAS ≥ 1(C).*

A

Parameter	Estimated Value*		SEM*	
	Extension fast	Flexion fast	Extension fast	Flexion fast
m (kg)	0.89 (0.65-1.1)	0.96 (0.73-1.1)	0.012 (0.0094-0.016)	0.015 (0.010-0.019)
k_{ext} (1/m)	206 (164-313)	307 (227-441)	0.012 (0.0059-0.019)	0.023 (0.013-0.037)
k_{flex} (1/m)	211 (162-265)	218 (205-288)	0.0057 (0.0037-0.012)	0.0059 (0.0043-0.0097)
$l_{p,slack,ext}$ (m)	0.066 (0.058-0.072)	0.072 (0.065-0.076)	0.0045 (0.0028-0.0066)	0.0047 (0.0027-0.0082)
$l_{p,slack,flex}$ (m)	0.048 (0.038-0.052)	0.047 (0.043-0.055)	0.0039 (0.0032-0.0072)	0.0044 (0.0026-0.0086)
$l_{opt,ext}$ (m)	0.057 (0.050-0.066)	0.064 (0.054-0.072)	0.0066 (0.0031-0.025)	0.017 (0.0054-0.38)
$l_{opt,flex}$ (m)	0.067 (0.051-0.078)	0.070 (0.060-0.090)	0.0083 (0.0050-0.020)	0.023 (0.0077-0.093)
Tau_{rel} (s)	2.1 (0.79-3.5)	1.6 (0.74-4.0)	0.028 (0.010-0.058)	0.052 (0.018-0.14)
k_{rel} (-)	0.65 (0.48-1.3)	1.1 (0.64-2.2)	0.0098 (0.0054-0.019)	0.022 (0.0086-0.050)
G_{ext} (-)	5676 (1858-17038)	1756 (201-8411)	0.019 (0.0070-0.22)	0.025 (0.0041-0.27)
G_{flex} (-)	15192 (5280-62793)	35866 (4764-112308)	0.071 (0.021-0.16)	0.22 (0.042-0.94)
f_0 (Hz)	0.19 (0.062-0.52)	0.19 (0.072-0.67)	0.012 (0.0039-0.028)	0.019 (0.0042-0.067)

* median, 25-75 percentile

B

Parameter	Estimated Value*		SEM*	
	Extension fast	Flexion fast	Extension fast	Flexion fast
m (kg)	1.4 (1.0-2.0)	1.1 (0.72-1.6)	0.040 (0.022-0.052)	0.034 (0.021-0.053)
k_{ext} (1/m)	207 (155-253)	244 (207-287)	0.019 (0.011-0.040)	0.025 (0.014-0.034)
k_{flex} (1/m)	204 (171-235)	215 (198-280)	0.010 (0.008-0.016)	0.011 (0.0076-0.019)
$l_{p,slack,ext}$ (m)	0.065 (0.056-0.070)	0.067 (0.062-0.073)	0.0092 (0.0050-0.016)	0.0084 (0.0053-0.013)
$l_{p,slack,flex}$ (m)	0.046 (0.040-0.050)	0.048 (0.042-0.055)	0.0098 (0.0055-0.013)	0.0076 (0.0048-0.014)
$l_{opt,ext}$ (m)	0.064 (0.053-0.084)	0.068 (0.058-0.095)	0.026 (0.011-0.11)	0.024 (0.012-0.14)
$l_{opt,flex}$ (m)	0.059 (0.050-0.069)	0.064 (0.056-0.11)	0.0098 (0.0051-0.045)	0.022-0.0079-0.18)
Tau_{rel} (s)	0.87 (0.57-1.2)	0.69 (0.47-1.5)	0.026 (0.012-0.037)	0.019 (0.014-0.060)
k_{rel} (-)	0.95 (0.66-1.9)	1.3 (0.66-2.2)	0.025 (0.016-0.050)	0.037 (0.012-0.068)
G_{ext} (-)	3285 (550-11671)	2147 (668-8556)	0.031 (0.0080-0.23)	0.040 (0.0092-0.19)
G_{flex} (-)	12534 (5499-29479)	10440 (5908-32914)	0.050 (0.016-0.27)	0.087 (0.032-1.8)
f_0 (Hz)	0.68 (0.14-1.3)	0.83 (0.22-2.0)	0.080 (0.031-0.12)	0.084 (0.037-0.18)

* median, 25-75 percentile

C

Parameter	Estimated Value*		SEM*	
	Extension fast	Flexion fast	Extension fast	Flexion fast
m (kg)	0.50 (0.50-1.5)	0.97 (0.50-1.4)	0.069 (0.035-0.090)	0.037 (0.026-0.061)
k_{ext} (1/m)	253 (174-303)	220 (167-277)	0.028 (0.011-0.057)	0.023 (0.012-0.028)
k_{flex} (1/m)	167 (130-209)	178 (134-256)	0.0090 (0.0045-0.015)	0.0085 (0.0057-0.013)
$l_{p,slack,ext,}$ (m)	0.066 (0.058-0.073)	0.064 (0.059-0.069)	0.0084 (0.0050-0.016)	0.0085 (0.0049-0.016)
$l_{p,slack,flex}$ (m)	0.027 (0.012-0.035)	0.035 (0.019-0.044)	0.013 (0.0079-0.019)	0.0079 (0.0058-0.015)
$l_{opt,ext}$ (m)	0.059 (0.042-0.11)	0.066 (0.054-0.10)	0.038 (0.015-0.077)	0.045 (0.014-0.18)
$l_{opt,flex}$ (m)	0.054 (0.050-0.060)	0.057 (0.048-0.092)	0.0056 (0.0038-0.011)	0.0096 (0.0048-0.11)
Tau_{rel} (s)	1.1 (0.81-1.9)	1.3 (0.87-2.2)	0.020 (0.014-0.032)	0.030 (0.019-0.043)
k_{rel} (-)	2.2 (1.1-3.5)	1.4 (0.97-2.2)	0.031 (0.020-0.10)	0.029 (0.018-0.042)
G_{ext} (-)	50920 (13062-125798)	12023 (3627-36043)	1.6 (0.35-5.9)	0.42 (0.11-1.8)
G_{flex} (-)	15010 (7010-22856)	15134 (7540-26495)	0.045 (0.017-0.088)	0.044 (0.020-0.81)
f_0 (Hz)	0.72 (0.29-1.0)	0.33 (0.20-0.56)	0.043 (0.022-0.10)	0.042 (0.024-0.071)

* median, 25-75 percentile

Validity and agreement

<u>Model fit and parameter confidence</u>

Estimated values of model parameters and SEM values are presented in Table 4.3 for "extension fast" and "flexion fast" direction for all healthy subjects and stroke patients with MAS = 0 and MAS ≥ 1, i.e. without excluding data based on low VAF values. The median VAF for the "extension fast" were 99.6 (interquartile range (*IQR*): 99.4 - 99.7)%, 99.5 (*IQR:* 98.9-99.8)% and 99.8 (*IQR:* 99.6-99.9)% for healthy subjects, patients with MAS = 0 and patients with MAS ≥ 1 respectively and for "flexion fast" direction 99.3 (*IQR:* 98.1 - 99.7)%, 99.5 (*IQR:* 98.5-99.7)%.and 99.8 (*IQR:* 99.7-99.9)%. Median SEM values were lower than 0.1, except for G_{flex} for "flexion fast" (0.22) for healthy subjects and G_{ext} for both movement directions (1.6 and 0.42) for patients with MAS ≥ 1.

<u>Assessment of systematic error</u>

We observed no significant differences for almost all outcome parameters between the measurements of two different visits based on the Wilcoxon signed rank test, indicating that no systematic error between measurements was present for these parameters. One exception was observed for the reflexive torque T_{reflex} of the flexors in "flexion fast" direction (P=0.022).

Clinical potential

Figure 4.4 shows the results of the comparison between healthy controls and patients with MAS = 0 and MAS ≥ 1 score. Patients with MAS ≥ 1, MAS = 0 and healthy controls significantly differed for tissue stiffness, K_{joint} (P=0.0023 "extension fast"; P=0.0020 "flexion fast"), reflexive torque, T_{reflex} of the flexors (P=0.0011 "extension fast"; P=0.014 "flexion fast"), optimal muscle length, l_{opt} of the flexors (P=0.047 "extension fast") and slack muscle length, $l_{p,slack}$ of the flexors (P=0.0031 "extension fast"; P=0.0177 "flexion fast") and extensors (P=0.020 for "flexion fast"). Multiple comparison showed significant differences between patients with MAS ≥ 1 and healthy controls for K_{joint} (both movement directions), T_{reflex} of the flexors ("extension fast"), l_{opt} of the flexors and $l_{p,slack}$ of the flexors (both movement directions) and extensors. Between MAS = 0 and MAS ≥ 1 significant differences were found for K_{joint} (both movement directions), T_{reflex} of the flexors (both movement directions) and $l_{p,slack}$ of the flexors ("extension fast"). Healthy subjects and stroke patients with MAS = 0 did not differ.

When using the MDC, ten patients had a deviated K_{joint} value (≥3.13 Nm/rad, MDC=1.79 Nm/rad) in "extension fast" direction, eight patients a deviated K_{joint} (≥3.45 Nm/rad; MDC=2.34 Nm/rad) in the "flexion fast" direction and ten patients a deviated T_{reflex} of the flexor muscles (≥ 0.72 Nm; MDC=0.457 Nm) in "extension fast" direction. Almost all of these patients had a MAS ≥ 1: 9 out of 10 for K_{joint} in "extension fast" direction, 8 out of 8 for K_{joint} in "flexion fast" direction and 8 out of 10 for T_{reflex} of the flexors in "extension fast" direction. For the "extension fast" direction 9 out of 11 patients had an increased K_{joint} together with an increased T_{reflex} of the FCR. All patients that showed an increased K_{joint} in the "flexion fast" direction had an increased K_{joint} in the "extension fast" direction.
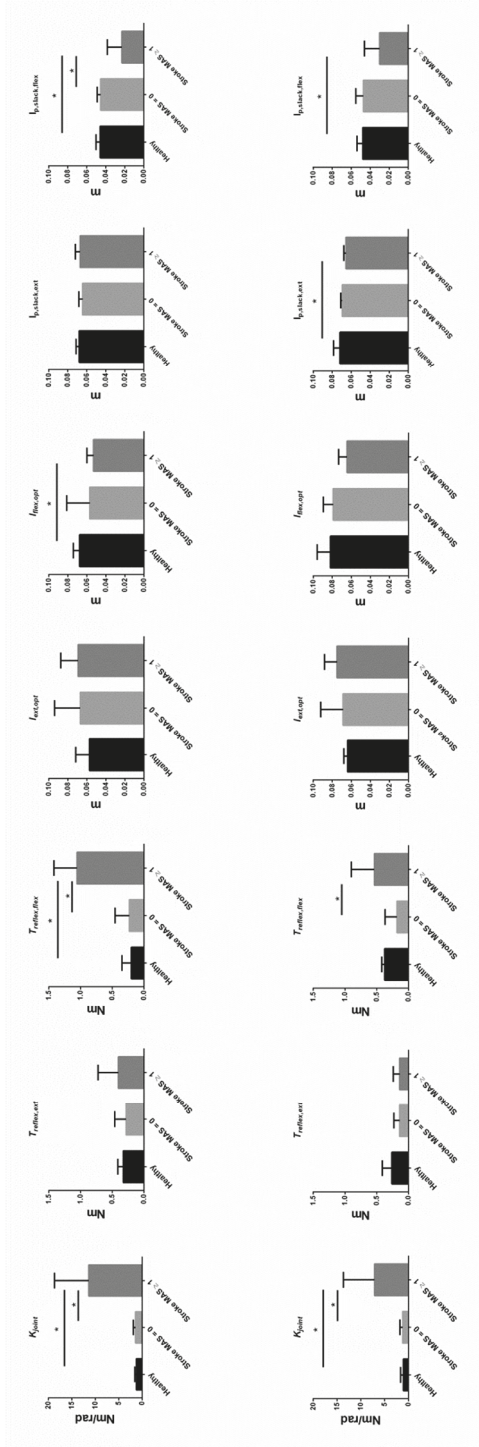
Figure 4.4: Outcome measures (median with interquartile range) for "extension.fast" (top) and "flexion.fast" (bottom) direction for healthy subjects and patients with stroke with MAS = 0 and MAS ≥ 1. Asterisks denote significant differences between groups.

Discussion

Neural and non-neural outcome parameters including optimal muscle length and slack length of connective tissue were quantitatively assessed for the wrist joint in a cohort of chronic stroke patients using an EMG driven antagonistic muscle model. High VAF values and low SEM illustrated the validity of the model approach. Differences in tissue stiffness, reflexive torque, optimal muscle length and slack length of connective tissues between patients with MAS score ≥ 1 and healthy controls demonstrated clinical potential of the method.

Validity and agreement

We advocate the use of an EMG driven model because non-invasive techniques to estimate the physiological parameters are yet lacking. This imposes both the quest for validation and the implicit inability to do so. Three demands were imposed to the model: The structure of the model should represent the (non-linear) joint physiology, the predicted torques should resemble the measured torques and the parameters should be sensitive to discriminate clinical different patients from healthy volunteers.

Model fit and parameter confidence

The model structure was able to describe the relation between joint position and EMG input and the torque output as indicated by the high variance accounted for (VAF) of 98% or higher in 90% of the cases) in the healthy group and both stroke groups.

The model contains 12 parameters. Sensitivity and the absence of parameter redundancy within the model were checked using the standard error of the mean (SEM). The estimation of the model parameters was sufficiently accurate indicated by the low SEM values (Table 4.3).

The SEM for the gain factor G_{flex} for "flexion fast" (0.22) in healthy subjects and the SEM for the gain factor G_{ext} in "extension fast" (1.6) and "flexion fast" (0.42) was largest. These scaling factors are essential in relating muscle activation with torque, but only relevant in case of sufficient (reflexive) activation, explaining the relatively high SEM for G_{flex} for the "flexion fast" direction and G_{ext} for the "extension fast" direction.

Assessment of systematic error

There was no systematic error between measurements at two different visits except for the the reflexive torque, T_{reflex} of the flexors in "flexion fast" direction, possibly due to varying muscle activity in stroke patients. This was confirmed by systematic error assessment between measurements of two different visits for T_{reflex} of the flexors for healthy subjects ($P=0.314$) and stroke patients ($P=0.033$) separately.

Clinical potential: Increased neural and structural contributors of joint stiffness in stroke

Patients with MAS $\geq$ 1 differed from healthy controls in neural (T_{reflex}) and non-neural or structural (K_{joint}, $l_{opt,m}$ and $l_{p,slack,m}$) parameters. The decrease in optimal muscle length (l_{opt}) and muscle slack length ($l_{p,slack}$) of the flexor muscles indicates a shift in the active and passive force-length relationship. Functionally, this structural change implies a flexed joint rest position with a smaller RoM for the impaired wrist, the latter confirmed by a previous study on the same cohort[25] where the authors found significant differences for the passive and active RoM between MAS $\geq$ 1 and both the MAS = 0 and healthy group. However, van der Krogt et al.[25] could not establish a significant change in the passive angle at rest (angle at zero torque), which could be explained by the influence of active components (e.g. muscle tone) which could have resulted in a rest angle comparable to healthy controls.

When using the MDC, ten patients had a deviating tissue stiffness, K_{joint} and ten patients had a deviating reflexive torque, T_{reflex} of the flexor muscles in "extension fast" direction. Nine of these eleven patients with deviated outcome measures had a MAS score $\geq$ 1. One patient with MAS $\geq$ 1 (for flexor muscles) score showed tissue stiffness and reflexive torque values within the range observed in healthy subjects. Differences between patients in outcome measures indicate that there may be a large variety in the neural and non-neural characteristics in stroke patients as also shown by the variation in the MAS.

Nine out of the eleven identified patients had an increased K_{joint} together with an increased T_{reflex} of the flexors. Increased values for both K_{joint} and T_{reflex} are comparable with results found for the ankle where K_{joint} and T_{reflex} were also both increased with elevated MAS[9]. This is in contrast with results in cerebral palsy where a large variation was found between the neural (reflexive torque of triceps surae) and structural (tissue stiffness of triceps surae) contributors of joint stiffness in the ankle[10;11]. This variation in the manifestation of neural and non-neural

contributors suggests a different mechanism in development of increased joint stiffness in stroke and cerebral palsy.

Estimation of optimal muscle length and slack muscle length

Parameters represent physiology of subjects but these in vivo estimated parameters for lumped muscle groups cannot directly be related to muscular parameter values as muscle activation dynamics (slow and fast fibre types) and muscle structure (e.g. pennation angle, muscle and tendon) is not exactly represented. The goal of this model is to systematically discriminate neural contributions from secondary structural changes in connective and contractile tissue observed in patients with upper neuron motor diseases like stroke. The exact value for the outcome measures can be different with literature, but the values and changes need to be of the same order of magnitude.

In literature an optimal fiber length of 0.064-0.099 m was reported for the ECR[35-41] and 0.081 m and 0.059 m for the ECR longus and brevis[42-44]. An optimal fiber length of 0.052-0.080 m was reported for the FCR[35-42;44]. A fiber length of 0.076 m and 0.048 m was reported for the ECRL and ECRB and 0.051 m for the FCR[42]. Our optimal length and slack length were in the same order of magnitude as the parameters in literature (median l_{opt} of 0.061 m and 0.071 m for extensor and flexor muscles respectively; median $l_{p,slack}$ of 0.069 m for the extensors and 0.047 m for the flexors).

The estimated l_{opt} and $l_{p,slack}$ of the flexors of the MAS $\geq$ 1 group were smaller compared to the values for healthy controls indicating that the range the flexor can generate force is reduced and connective tissue is stiffer and shortened. By uncoupling the slack muscle length and optimal muscle length we allow the model to estimate the passive and active characteristics of the muscle independently. Physiologically, the parameters may be related. E.g. longer sarcomeres, i.e. less sarcomeres in series, result in higher passive stiffness through the intrinsic fiber skeletal properties. However, an increase in extracellular matrix stiffness, described in children with cerebral palsy[18], results in a decoupled increase of passive stiffness: the slack muscle length becomes smaller while the optimal muscle length remains unchanged.

Clinical implication

Patients with MAS ≥ 1 can be discriminated from healthy controls and patients with MAS = 0 by neural and non-neural contributors of joint stiffness using the presented bidirectional EMG driven model describing the position and force signals including EMG obtained with a wrist manipulator at high temporal resolution. We now have a method to study longitudinal changes of the neuromuscular system and the effect of treatment, like botulinum toxin injections, on the different neural and non-neural contributors of joint stiffness. Individual stroke patients with deviated tissue stiffness and reflexive torque can be discriminated from healthy controls using the minimal detectable change (MDC). This method gives the clinician the opportunity to monitor the different components of joint stiffness in time and to adjust treatment in individual stroke patients.

The mechanism of muscle shortening after an upper motor neuron disease is not yet understood[16]. Longitudinal observation of the neural and non-neural contributors of joint stiffness, including the estimation of parameters representing the optimal muscle length and slack length of connective tissue, in the acute and sub-acute phase post-stroke and during ageing in children with cerebral palsy, could be of great value to e.g. better understand the mechanism of development of structural changes after a neural lesion.

Limitations

The wrist was rotated over its full RoM in one second to approximate the clinical Ashworth test. Because RoM in patients was generally reduced, movement velocity for the stroke patients was lower as compared to the healthy group. As stretch reflexes are velocity dependent reflexive muscle forces in the patients may even have been underestimated compared to the observations in the healthy group.

Optimal muscle length is a characteristic observable only in the active muscles, while the presented data are measured during a passive task. There was generally sufficient muscle activity present to estimate the optimal muscle length in a valid way as demonstrated by the SEM values (median SEM value <0.05 for optimal muscle length for all conditions). Additional active tasks should be considered to ensure sufficient muscle activation to estimate the optimal muscle length in all cases.

10% of the trials were rejected based on VAFs lower than 98%. In only one (out of 45) subject, the parameters could not be estimated because the patient had low VAF values in both movement direction and for both trials. From all other subjects, in repeated trials in flexion or extension, data became available to estimate the relevant parameters. Repetition of trials is therefore recommended. The constraint of VAF to be larger than 98% in order to approve trials was quite strict to ensure sufficient quality of the model fits. Low VAF values may have originated from experimental artefacts or voluntary interaction with the passive protocol.

In our model the moment arms and muscle lengths at zero degrees wrist angle position of the ECR longus and brevis are averaged which is a simplification of reality[45]. Furthermore, as the torque measured is the result of all extensor and flexor muscles, the modeled extensor and flexor muscle elements are lumped descriptions of the wrist muscles affecting the wrist flexion and extension torques (e.g. extensor carpi ulnaris, flexor carpi ulnaris). The characteristics of the ECR and FCR were used as initial parameter values for the corresponding muscle elements. Pennation angles were not included in the model, i.e. pennation angles were defined zero and consequently muscle and fiber length were defined to be equal. Since pennation angle changes the relationship between muscle length and force, the outcome parameters may be biased by this assumption. However, as this is the case in all subjects, differences in optimal muscle length and slack muscle length, parameterized by $l_{opt,m}$ and $l_{p,slack,m}$ are assumed to represent physiological adaptation of the neuromuscular system and although the model is a simplification of the wrist joint it appeared to be sensitive to evaluate changes after stroke.

Conclusions

The EMG driven model in combination with the applied ramp-and-hold movements in both patients and healthy controls enabled us to estimate parameters representing tissue stiffness, reflexive torques, optimal muscle lengths and slack muscle lengths of connective tissue at the wrist in rest. Patients with an elevated MAS (MAS ≥ 1) were distinguished from healthy controls and patients with MAS = 0. Patients with MAS ≥ 1 differed from healthy controls through increased tissue stiffness and reflexive torque and reduced optimal muscle length and slack length of flexor connective tissue. The differentiation of joint stiffness into different neural and structural components is essential for individualized treatment selection in patients with upper motor neuron diseases and will be of benefit to follow the disease in time in acute

and sub-acute stroke patients and during ageing in children with cerebral palsy. Validation remains a point of attention in future applications. Next studies will focus on the effect of botulinum toxin treatment in chronic stroke patients and the quantification of joint stiffness during the acute and sub-acute phase of stroke.

Acknowledgments

References

(1) Dietz V, Sinkjaer T. Spastic movement disorder: impaired reflex function and altered muscle mechanics. *Lancet Neurol* 2007;6:725-733.

(2) van der Krogt HJ, Meskers CG, de Groot JH, Klomp A, Arendzen JH. The gap between clinical gaze and systematic assessment of movement disorders after stroke. *J Neuroeng Rehabil* 2012;9:61.

(3) Bar-On L, Molenaers G, Aertbelien E et al. Spasticity and its contribution to hypertonia in cerebral palsy. *Biomed Res Int* 2015;2015:317047.

(4) Sheean G. Botulinum toxin should be first-line treatment for poststroke spasticity. *J Neurol Neurosurg Psychiatry* 2009;80:359.

(5) Gracies JM, Singer BJ, Dunne JW. The role of botulinum toxin injections in the management of muscle overactivity of the lower limb. *Disabil Rehabil* 2007;29:1789-1805.

(6) Thompson AJ, Jarrett L, Lockley L, Marsden J, Stevenson VL. Clinical management of spasticity. *J Neurol Neurosurg Psychiatry* 2005;76:459-463.

(7) Mortenson PA, Eng JJ. The use of casts in the management of joint mobility and hypertonia following brain injury in adults: a systematic review. *Phys Ther* 2003;83:648-658.

(8)   Renzenbrink GJ, Buurke JH, Nene AV, Geurts AC, Kwakkel G, Rietman JS. Improving walking capacity by surgical correction of equinovarus foot deformity in adult patients with stroke or traumatic brain injury: a systematic review. *J Rehabil Med* 2012;44:614-623.

(9)   de Vlugt E, de Groot JH, Schenkeveld KE, Arendzen JH, van der Helm FC, Meskers CG. The relation between neuromechanical parameters and Ashworth score in stroke patients. *J Neuroeng Rehabil* 2010;7:35.

(10)   de Gooijer-van de Groep KL, de Vlugt E, de Groot JH et al. Differentiation between non-neural and neural contributors to ankle joint stiffness in cerebral palsy. *J Neuroeng Rehabil* 2013;10:81.

(11)   Sloot LH, van der Krogt MM, de Gooijer-van de Groep KL et al. The validity and reliability of modelled neural and tissue properties of the ankle muscles in children with cerebral palsy. *Gait Posture* 2015.

(12)   Parker VM, Wade DT, Langton HR. Loss of arm function after stroke: measurement, frequency, and recovery. *Int Rehabil Med* 1986;8:69-73.

(13)   Broeks JG, Lankhorst GJ, Rumping K, Prevo AJ. The long-term outcome of arm function after stroke: results of a follow-up study. *Disabil Rehabil* 1999;21:357-364.

(14)   Malhotra S, Pandyan AD, Rosewilliam S, Roffe C, Hermens H. Spasticity and contractures at the wrist after stroke: time course of development and their association with functional recovery of the upper limb. *Clin Rehabil* 2011;25:184-191.

(15)   Lieber RL, Friden J. Spasticity causes a fundamental rearrangement of muscle-joint interaction. *Muscle Nerve* 2002;25:265-270.

(16)   Lieber RL, Steinman S, Barash IA, Chambers H. Structural and functional changes in spastic skeletal muscle. *Muscle Nerve* 2004;29:615-627.

(17)   Gao F, Zhang LQ. Altered contractile properties of the gastrocnemius muscle poststroke. *J Appl Physiol (1985)* 2008;105:1802-1808.

(18)   Smith LR, Lee KS, Ward SR, Chambers HG, Lieber RL. Hamstring contractures in children with spastic cerebral palsy result from a stiffer extracellular matrix and increased in vivo sarcomere length. *J Physiol* 2011;589:2625-2639.

(19)   Ada L, Canning CG, Low SL. Stroke patients have selective muscle weakness in shortened range. *Brain* 2003;126:724-731.

(20) Hu X, Tong K, Tsang VS, Song R. Joint-angle-dependent neuromuscular dysfunctions at the wrist in persons after stroke. *Arch Phys Med Rehabil* 2006;87:671-679.

(21) Kwakkel G, Meskers CG, van Wegen EE et al. Impact of early applied upper limb stimulation: the EXPLICIT-stroke programme design. *BMC Neurol* 2008;8:49.

(22) Mirbagheri MM, Rymer WZ. Time-course of changes in arm impairment after stroke: variables predicting motor recovery over 12 months. *Arch Phys Med Rehabil* 2008;89:1507-1513.

(23) Kwakkel G, Meskers CG. Botulinum toxin A for upper limb spasticity. *Lancet Neurol* 2015.

(24) Klomp A, van der Krogt JM, Meskers CGM et al. Design of a concise and comprehensive protocol for post stroke neuromechanical assessment. *J Bioengineer & Biomedical Sci* 2012.

(25) van der Krogt HJ, Klomp A, de Groot JH et al. Comprehensive neuromechanical assessment in stroke patients: reliability and responsiveness of a protocol to measure neural and non-neural wrist properties. *J Neuroeng Rehabil* 2015;12.

(26) Instrumented Stretch Reflexes of Flexor Carpi Radialis and Flexor Carpi Ulnaris Muscle. XVIth ISEK Conference; 06 Jun 29; 2006.

(27) Hodson-Tole EF, Loram ID, Vieira TM. Myoelectric activity along human gastrocnemius medialis: different spatial distributions of postural and electrically elicited surface potentials. *J Electromyogr Kinesiol* 2013;23:43-50.

(28) Ramsay JW, Hunter BV, Gonzalez RV. Muscle moment arm and normalized moment contributions as reference data for musculoskeletal elbow and wrist joint models. *J Biomech* 2009;42:463-473.

(29) Winters JM. An improved muscle-reflex actuator for use in large-scale neuro-musculoskeletal models. *Ann Biomed Eng* 1995;23:359-374.

(30) Thelen DG. Adjustment of muscle mechanics model parameters to simulate dynamic contractions in older adults. *J Biomech Eng* 2003;125:70-77.

(31) de Vlugt E, de Groot JH, Wisman WH, Meskers CG. Clonus is explained from increased reflex gain and enlarged tissue viscoelasticity. *J Biomech* 2011.

(32) de Vet HC, Terwee CB, Knol DL, Bouter LM. When to use agreement versus reliability measures. *J Clin Epidemiol* 2006;59:1033-1039.

(33) Ljung L. *System identification - Theory for the user*. Prentice Hall, 1999.

(34) Haley SM, Fragala-Pinkham MA. Interpreting change scores of tests and measures used in physical therapy. *Phys Ther* 2006;86:735-743.

(35) Amis AA, Dowson D, Wright V. Muscle strengths and musculoskeletal geometry of the upper limb. *Eng Med (Berlin)* 1979;8:41-48.

(36) An KN, Hui FC, Morrey BF, Linscheid RL, Chao EY. Muscles across the elbow joint: a biomechanical analysis. *J Biomech* 1981;14:659-669.

(37) Brand PW, Beach RB, Thompson DE. Relative tension and potential excursion of muscles in the forearm and hand. *J Hand Surg Am* 1981;6:209-219.

(38) Winters JM, Stark L. Estimated mechanical properties of synergistic muscles involved in movements of a variety of human joints. *J Biomech* 1988;21:1027-1041.

(39) Cutts A, Alexander RM, Ker RF. Ratios of cross-sectional areas of muscles and their tendons in a healthy human forearm. *J Anat* 1991;176:133-137.

(40) Loren GJ, Shoemaker SD, Burkholder TJ, Jacobson MD, Friden J, Lieber RL. Human wrist motors: biomechanical design and application to tendon transfers. *J Biomech* 1996;29:331-342.

(41) Garner BA, Pandy MG. Estimation of musculotendon properties in the human upper limb. *Ann Biomed Eng* 2003;31:207-220.

(42) Lieber RL, Fazeli BM, Botte MJ. Architecture of selected wrist flexor and extensor muscles. *J Hand Surg Am* 1990;15:244-250.

(43) Murray WM, Buchanan TS, Delp SL. The isometric functional capacity of muscles that cross the elbow. *J Biomech* 2000;33:943-952.

(44) Holzbaur KR, Murray WM, Delp SL. A model of the upper extremity for simulating musculoskeletal surgery and analyzing neuromuscular control. *Ann Biomed Eng* 2005;33:829-840.

(45) Lieber RL, Ljung BO, Friden J. Intraoperative sarcomere length measurements reveal differential design of human wrist extensor muscles. *J Exp Biol* 1997;200:19-25.

Appendix 4: Wrist model

The model structure was based on the ankle model from de Vlugt et al.[1] and adapted to the neuromechanical characteristics of the wrist joint. The following structure aspects were added in the wrist model compared to the ankle model: Optimal muscle length parameters were estimated, the stiffness components were modeled for both flexor and extensor muscles making the model fully bi-directional and tissue relaxation was included. Model parameters are listed in Table 4.2.

Wrist joint stiffness is described by:

$$T_{mod}(t) = I\ddot{\theta}(t) + T_{ext}(t) - T_{flex}(t) \qquad (A4.1)$$

where t is the independent time variable [s], T_{mod} the modeled wrist reaction torque [Nm], $I\ddot{\theta}(t)$ the wrist angular acceleration [rad/s²], I the inertia of wrist and handle [kg.m²], T_{ext} the torque generated by the extensor muscles [Nm] and T_{flex} the torque generated by the flexor muscles [Nm].

Muscle torques (T_m) for extensor and flexor muscle are described by:

$$T_m(\theta,t) = (F_{elas,m}(l) + F_{act,m}(v_m, l_m, \alpha_m))r_m(\theta) \qquad (A4.2)$$

with $F_{elas,m}$ the elastic force of the parallel connective tissues [N], $F_{act,m}$ the active or "reflexive" muscle forces [N] according to the Hill-type model, v_m the muscle lengthening velocity [m/s], l_m the muscle length [m], α_m the active state [-] and $r_m(\theta)$ the angle dependent moment arm [m] of the tendon.

The ECR and FCR were used as representation of the extensor and flexor muscles. The moment arms [m] of the ECR and FCR muscles are dependent on the angular position of the joint and defined using the equations of Ramsay et al.[2]:

$$r_{FCR}(\theta) = 13.2040 + 1.5995\theta \quad \text{for} \quad \theta > -10° \quad [\text{x}10^{-3}m] \qquad (A4.3)$$

$$r_{ECR,brevis}(\theta) = 13.4337 - 2.1411\theta \ \text{ for } \ \theta < 10° \ [\text{x}10^{-3}m] \qquad (A4.4)$$

$$r_{ECR,longus}(\theta) = 11.7166 - 2.2850\theta \ \text{ for } \ \theta < 10° \ [\text{x}10^{-3}m] \qquad (A4.5)$$

$$r_{ECR}(\theta) = (r_{ECR,brevis}(\theta) + r_{ECR,longus}(\theta))/2 \qquad (A4.6)$$

The ECR is in fact two separate muscles: the extensor carpi radialis longus and brevis. Since only a combined EMG signal can be measured the extensor moment arm is assumed to be the average of the two separate moment arms. Muscle length equals:

$$l_{FCR} = l_{FCR,0} - r_{FCR}(\theta)\theta \qquad (A4.7)$$

$$l_{ECR} = l_{ECR,0} + r_{ECR}(\theta)\theta \qquad (A4.8)$$

Where l_{FCR} and l_{ECR} are the lengths of the muscle at each position θ and $l_{FCR,0}$ and $l_{ECR,0}$ the muscle length at zero degrees wrist angle position (handle in line with the forearm). The zero muscle lengths are $l_{FCR,0}$ = 6.3 cm and $l_{ECR,0}$ = 7.0 cm (average of ECR longus and brevis, optimal fiber lengths from[3-5]. $r_{FCR}(\theta)\theta$ and $r_{ECR}(\theta)\theta$ are the arc lengths of the tendon that stretches around the joint bone when the joint rotates about angle θ [6]. Positive angles represent flexion, thus the flexor muscles shorten during flexion and the extensor muscles lengthen during flexion, and vice versa for extension.

Inertia of hand and the handle is modeled as a point mass m [kg] at distance l_a (fixed at 0.1 m) from the axis of rotation:

$$I = ml_a^2 \ [\text{kg.m}^2] \qquad (A4.9)$$

The elastic components for the extensor and flexor muscles were modeled as follows:

$$F_{elas,m}(t) = e^{k_m(l_m(\theta) - l_{p,slack,m})} \qquad (A4.10)$$

Where k_m is the estimated stiffness coefficient of the muscle and $l_{p,slack,m}$ the estimated slack length of the connective tissue. Muscle connective tissue under tension exhibits relaxation or force decrease[7-9], which is modeled by a first order filter, according to:

$$F_{elas,m}(s) = \frac{\tau_{rel}s + 1}{\tau_{rel}s + 1 + k_{rel}} F_{elas,m}(s) \tag{A4.11}$$

with τ_{rel} the estimated tissue relaxation time constant and k_{rel} the estimated tissue relaxation factor. In the previous version of the model by de Vlugt et al.[1] tissue relaxation was approximated by a viscous damper.

For clinical comparison between subjects, tissue stiffness at joint level, K_{joint}, was compared at the same wrist angle (θ_{comp}) for all subjects. This angle was chosen at zero degrees, i.e. where the handle is in line with the forearm.

$$K_{jo\,int,m} = k_m e^{k_m(l_{m,comp} - l_{p,slack,m})} r_m^2(\theta_{comp}) \quad \text{for } \theta_{comp} = 0 \text{ degrees} \tag{A4.12}$$

where $l_{m,comp}$ is the muscle length at θ_{comp}. Eq. (A4.12) was obtained by differentiation of Eq. (A4.10) with respect to muscle length and multiplied by the squared moment arm. The total tissue stiffness at joint level was derived by summation of the stiffness from both muscles:

$$K_{joint} = K_{joint,ext} + K_{joint,flex} \tag{A4.13}$$

Neural muscle activity for the extensors and flexors due to stretch reflexes was estimated from corresponding EMG signals according to:

$$U_m(t) = G_m EMG_m(t) \qquad\qquad (A4.14)$$

with U the excitation input to the muscle model [1/Volt]; G_m the dimensionless EMG weight scaling factor and EMG_m the average of the recorded EMG signal values of both muscle electrodes.

The neural excitations of both muscles were filtered with a linear second order filter to describe the activation process of a contracted muscle[1]:

$$\alpha_m(s) = \frac{\omega_0^2}{s^2 + 2\beta_m \omega_0 s + \omega_0^2} U_m(s) \qquad\qquad (A4.15)$$

α_m is the dimensionless active state of the muscle, $\omega_0 = 2\pi f_{0,m}$ the estimated cut off frequency of the activation filter, s the Laplace operator denoting the first time derivative and β_m the relative damping.

The Hill-type muscle model was used to compute the muscle force from the active state and the muscle length and velocity according to:

$$F_{act,m} = f_v(v_m) f_l(l, l_{opt,m}) \alpha_m \qquad\qquad (A4.16)$$

with f_v the force-velocity relationship and f_l the force-length relationship. The optimal muscle lengths ($l_{opt,m}$) were estimated using the model and used to derive the force-length relationships by

$$f_l = e^{-\left(l_m - l_{opt,m}\right)^2 / w_{fl,m}} \tag{A4.17}$$

With $w_{fl,m}$ a shape factor defined as:

$$w_{fl,m} = cf\, l_{opt,m}^{\,2} \tag{A4.18}$$

with *cf* the shape parameter of the force-length relationship with value 0.1 to resemble the force-generating range of the FCR and ECR[10;11]. The maximum shortening velocity was 8 times the optimal muscle length[12], the maximum eccentric force was 1.5 times the isometric force and the isometric force was normalized to 1 because the force had been scaled by the weighting factors G.

References

(1) de Vlugt E, de Groot JH, Schenkeveld KE, Arendzen JH, van der Helm FC, Meskers CG. The relation between neuromechanical parameters and Ashworth score in stroke patients. *J Neuroeng Rehabil* 2010;7:35.

(2) Ramsay JW, Hunter BV, Gonzalez RV. Muscle moment arm and normalized moment contributions as reference data for musculoskeletal elbow and wrist joint models. *J Biomech* 2009;42:463-473.

(3) Murray WM, Buchanan TS, Delp SL. The isometric functional capacity of muscles that cross the elbow. *J Biomech* 2000;33:943-952.

(4) Holzbaur KR, Murray WM, Delp SL. A model of the upper extremity for simulating musculoskeletal surgery and analyzing neuromuscular control. *Ann Biomed Eng* 2005;33:829-840.

(5) Lieber RL, Fazeli BM, Botte MJ. Architecture of selected wrist flexor and extensor muscles. *J Hand Surg Am* 1990;15:244-250.

(6) Lieber RL, Ljung BO, Friden J. Intraoperative sarcomere length measurements reveal differential design of human wrist extensor muscles. *J Exp Biol* 1997;200:19-25.

(7) Magnusson SP, Simonsen EB, Dyhre-Poulsen P, Aagaard P, Mohr T, Kjaer M. Viscoelastic stress relaxation during static stretch in human skeletal muscle in the absence of EMG activity. *Scand J Med Sci Sports* 1996;6:323-328.

(8) McNair PJ, Dombroski EW, Hewson DJ, Stanley SN. Stretching at the ankle joint: viscoelastic responses to holds and continuous passive motion. *Med Sci Sports Exerc* 2001;33:354-358.

(9) Bressel E, McNair PJ. The effect of prolonged static and cyclic stretching on ankle joint stiffness, torque relaxation, and gait in people with stroke. *Phys Ther* 2002;82:880-887.

(10) Garner BA, Pandy MG. Estimation of musculotendon properties in the human upper limb. *Ann Biomed Eng* 2003;31:207-220.

(11) Zajac FE. Muscle and tendon: properties, models, scaling, and application to biomechanics and motor control. *Crit Rev Biomed Eng* 1989;17:359-411.

(12) Thelen DG. Adjustment of muscle mechanics model parameters to simulate dynamic contractions in older adults. *J Biomech Eng* 2003;125:70-77.

4